International Journal of Mechanical Engineering

Structural and Optical Characterization of Nanostructured Zinc sulfide Thin Films deposited by CBD

Saja Faez Hassan
Department of Physics, College of Education, Mustansiriyah University, Iraq.

Oday Ali Chichan
Department of Physics, College of Education for Pure Sciences, University of Babylon, Iraq.

Zaid shaker abed mosa
Department of Pharmacy, Al-Manara College For Medical science, Iraq.

Sami Salman Chiad*
Department of Physics, College of Education, Mustansiriyah University, Iraq.

Nadir Fadhil Habubi
Department of Physics, College of Education, Mustansiriyah University, Iraq.

Abstract.

ZnS thin films were grown utilizing CBD method. ZnS films were deposited employing various molar concentrations of (1.0, 1.5 and 2.0) M at a temperature of 90 ºC. XRD profile offers an increment in grain size with the increment in molar concentration from 19.74 nm to 24.82 nm. Whilst the strain decreases from 17.55 to 13.96 with increase of molar concentration from (1.0 M and 2 M). AFM images show a fine surface morphology with rms roughness values decrease from 7.57 nm to 6.89 nm with the increment of molar concentration. The average diameter introduced by AFM was seen in the range of 92.74 nm to 86.54 nm with increase of molar content from 1.0 M and 2 M. The optical properties were studied by transmission spectra were found that for ZnS films have high transmittance in visible area is between 95 and 80 %, The absorption coefficient increased with increasing molarity from (1.0 M and 2 M). The bandgap offers a decrement from 3.55 eV to 3.35 eV with the increment in molarity.

Keywords: ZnS thin film, Structural properties, AFM, Optical properties, bandgap.

Introduction

ZnS is II–VI semiconductor , an n-type, whose bandgap was about 3.6 eV [1,2]. It was used as, LED [3], cathode-ray tubes [4], thin film electroluminescence [5], and buffer layers [6]. In general, ZnS occurs in two shape, cubic (zinc blende) and hexagonal (wurtzite) [7]. It is semiconductor with refractive index of (2.35) [8-11]. ZnS is utilized as window layer in solar cells [12-14]. ZnS is also used as a buffer layer [15-17]. Several techniques like sputtering [18], molecular beam epitaxy [19], PLD [20], CVD [21], SILAR [22], spray pyrolysis [23,55-75], and CBD [24-30] CBD can be employed as a large-area growth [31]. In the present work, CBD was employed to study some physical properties of nanostructured ZnS films utilizing various molar concentrations.

Experimental

ZnS thin films are deposited by CBD method on glass substrates (25mm x 50mm x 1mm). Zinc Sulphate of (1.0 , 1.5 and 2.0) M concentration in 25 ml of de-ionized water was employed. The glass substrates have been cleaned by first dipping for 30 minutes into HCl and HNO_3, cleaning in acetone with ultrasonic vibration for 20 minutes, inglorious into methanol solution, washed with de-ionized water, cleanly with (HF 5%). ZnS thin films were prepared by mixing 25ml of 0.25M zinc sulphate ($ZnSO_4$) as Zn^{2+} ion source, 25 ml of 3M hydrazine hydrate $(NH_2)_2$ and 25ml of 3M ammonia (NH_4OH) was employed as a complexing agent. The mixture immersed in the heated water bath with a temperature of 90°C, and stirred to guarantee homogeneous solution for 10 minutes. Thereafter, 50ml of 0.4M thiourea ($SC(NH_2)^2$) as S_2- ion source was added into the mixed solution with Zinc to Sulphur (Zn:S) molar ratio 1.0, 1.5, 2.0. Thereafter, the pre-clean bases were dipped vertically using substrate holder for 60 minutes. After completion film deposition. The films were removed and rinsed with redistilled water to take off soluble impurities and dried with N_2 gas. Thin, uniform and colorless ZnS films were obtained. The structural studies were done using X-ray diffractometer. AFM was employed to study film surface. Transmittance were recorded via double beam spectrophotometer (Schimadzu UV-probe 1650 Japan).

Results and Discussion

XRD styles are displayed in Fig. 1 show XRD pattern of ZnS film at 0.05M, can be observed appearing peaks at 2θ= 28.55°,47.51°, 56.28° and 69.52° which matched with (111), (220), (311) and (400) crystalline planes respectively, where the peak refer to the cubic ZnS phase. All the above mention planes refer to the polycrystalline ZnS with cubic phase. The diffraction intensity increases with increasing the molarity due to film thickness increasing and this implies a larger number of Bragg planes. The preferred peak was (111) plane and agree with the standard (ICDD No.05 -0566), it is obvious that, Bragg's peaks became more intense for higher molarity indicating a clear improvement in crystallinity. This behavior appreciably a constant procedure for all films were prepared by CBD as reported in literature [32, 33].

The grain size D of ZnS film was estimated via Scherrer's equation [34-36]:

$$D = \frac{0.9\,\lambda}{\beta cos\theta} \qquad (1)$$

Where λ is the wavelength of X-ray, □ is (FWHM) after making a suitable baseline correction.
The grain size was increased from 19. 74 nm to 24.82 nm with molarity increasing from 1.0 M to 2.0 M [35-38]. and the diffraction peaks become more strong and acute which marked that the grains be larger and the crystal fineness was enhanced. The variation in grain size could be attributed to cluster by cluster deposition and ion by ion deposition[7]. Table 1 shows that the strain(%) parameter decreases are (17.55 nm) to (13.96 nm) with molarity increasing from 1.0 M to 2.0 M thin films respectively,

The dislocation density (δ) was evaluated utilizing the equation below [37-40]:

$$\delta = \frac{1}{D^2} \qquad (2)$$

The lattice strain (ε) is evaluated using the equation below [41-43]:

$$\varepsilon = \frac{\beta cos\theta}{4} \qquad (3)$$

It can be seen that the value of ε (Table 1) increases With increasing with molarity increasing from 1.0 M to 2.0 M thin films respectively, Values of structural parameters are shown in Table. 1

Figure (2) displays FWHM, *D*, Dislocation density and Strain as a function of the prepared films, It notes the inverse relationship between Crystallite size and other parameters.

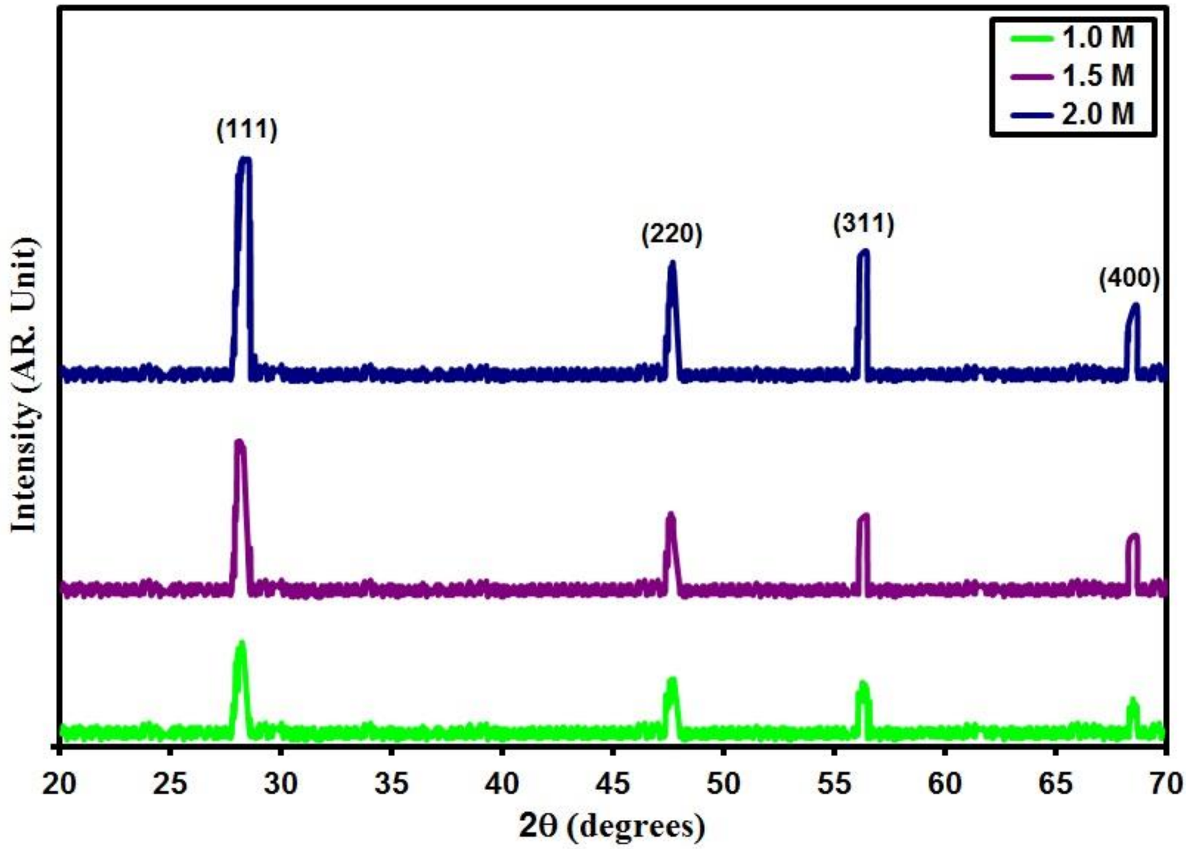

Fig.1. XRD styles of the prepared films.

Table 1. *D*, E_g and structural coefficient of the grown films.

Molar Observed	(hkl) Plane	2θ (°)	FWHM (°)	*D* (nm)	E_g (eV)	δ ($\times 10^{14}$)(lines/m^2)	ε ($x10^{-4}$)
1.0	111	28.55	0.39	19.74	3.55	25.66	17.55
1.5	111	28.37	0.37	21.15	3.45	22.35	15.65
2.0	111	28.05	0.33	24.82	3.35	16.23	13.96

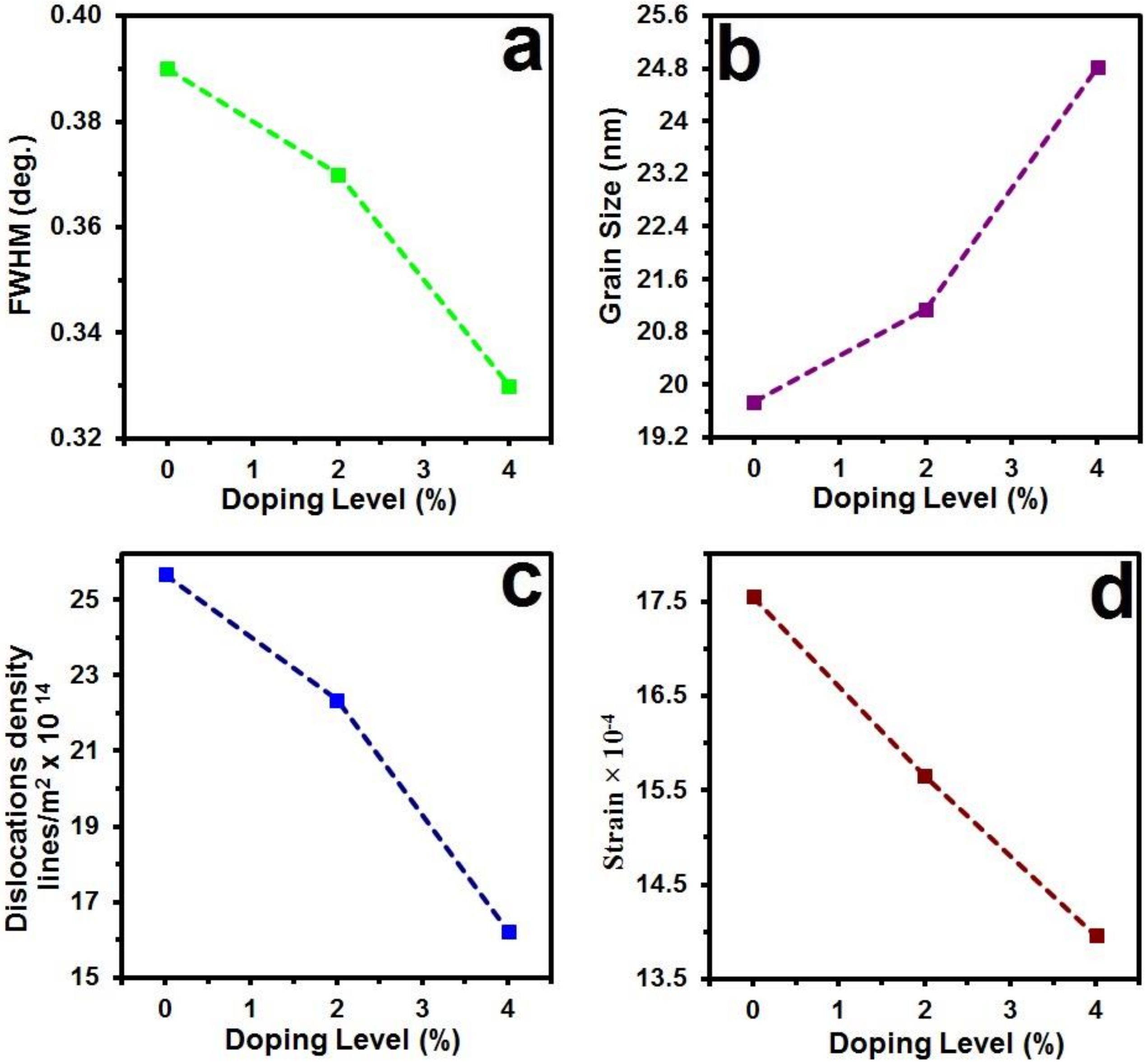

Fig. 2. FWHM (a) *D* (b) δ (c) ε (d) of the grown films.

Fig3. Shows AFM images to get surface features like root mean square (rms) or average roughness R Shown in Table 2. When taking two images with dimensions, Figure 3 (a_1, b_2 and c_1) 3D . Films are dole out orderly in the form of small granules. Figure 3 (a_2, b_2 and c_2) Shows curved volumetric distribution for crystalline granules where difference with molarity from 1.0 M ,1.5 M 2.0 M thin films respectively, From Figure 3 (a_3, b_3 and c_3). R and rms values of (7.57, 6.89 and 5.14) nm and (8.96, 8.09 and 6.00) nm, respectively, were determined for the surface roughness with molarity. The above analysis assure that R and rms are increase with molarity increased .
Table (2) offers AFM parameters A_P.

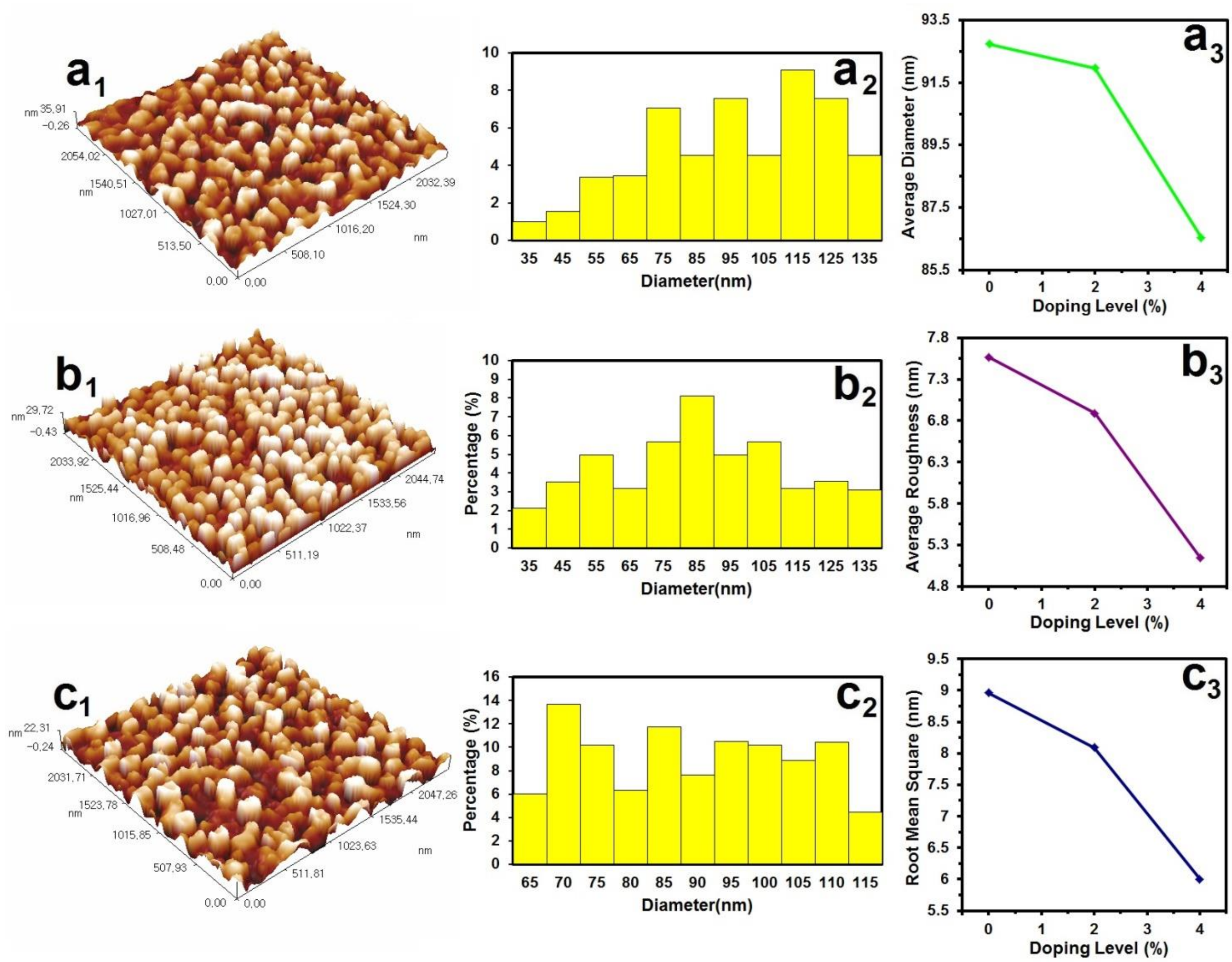

Fig.3. AFM images (a_1, b_1 and c_1), granularly distributed (a_2, b_2 and c_2) and A_P versus doping (a_3, b_3 and c_3).

Table 2. A_P of the grown films.

Molar Observed	Average Particle size nm	R (nm)	rms (nm)
1.0	92.74	7.57	8.96
1.5	91.97	6.89	8.09
2.0	86.54	5.14	6.00

Fig. 4. shows the transmittance T spectra. The maximum T was monitored at 95%, 85% and 80% for 1.0M, 1.5M and 2M respectively

The absorption coefficient (α) is specified by [44--46]:

$$\alpha = (2.303\times A)/t \qquad (4)$$

Where (t) is film thickness , A is absorbance. Fig. 5. displays α versus energy photon ($h\upsilon$) , films have ($\alpha > 10^4 cm^{-1}$) refereed to direct electronic transitions.

The bandgap energy E_g was determined by Tauc's relation [47-50]:

$$(\alpha h\nu) = \boldsymbol{A}(h\nu - E_g)^{\frac{1}{2}} \qquad (5)$$

where, **A** is a constant, A plot of $(\alpha h\nu)^2$ versus ($h\nu$) was displayed in Fig. 6. E_g of the intended films were 3.55 eV, 3.45 eV and 3.35 eV. These results agree with references [51-54].

Table (1) represent the values of E_g.

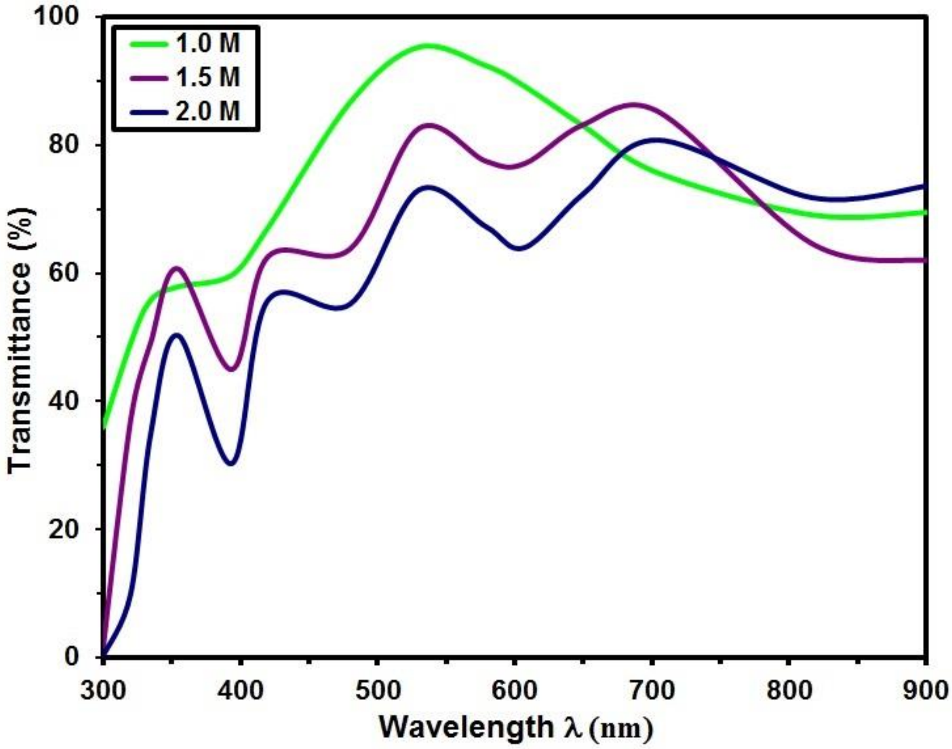

Fig.4. T of grown films.

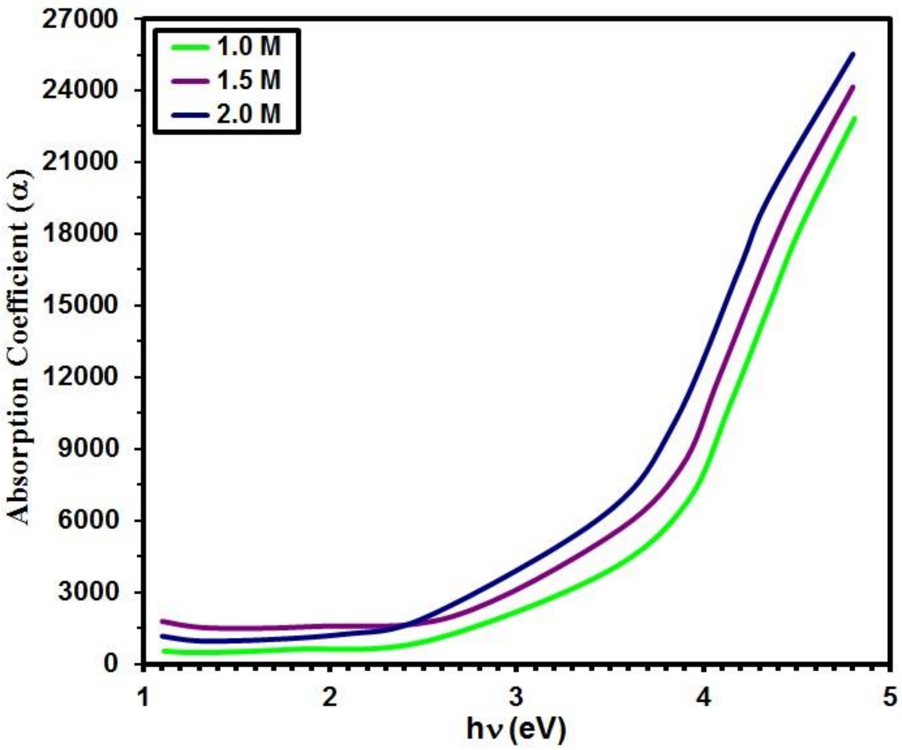

Fig. 5 α of grown films.

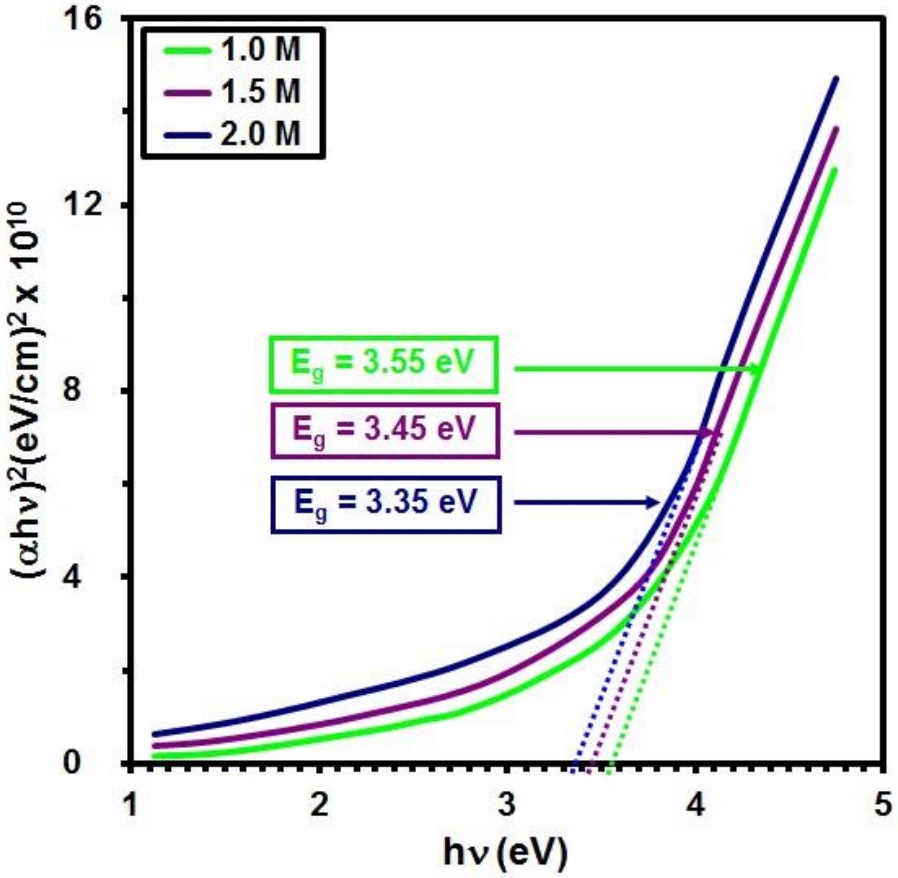

Fig. 6. $(\alpha h\nu)^2$ against hν of grown films.

Conclusion

ZnS thin film was grown utilizing CBD method. The XRD styles of the synthesized films offer a preferred orientation of (111) plane, *D* was increased from 19. 74 nm to 24.82 nm with molarity increasing from 1.0 M to 2.0 M, the strain parameter decreases are (17.55 nm) to (13.96 nm) with molarity increasing from 1.0 M to 2.0 M thin films respectively, AFM image offered that The grain size was noticed in the region of 92.74 nm to 86.54 nm for ZnS with increase of molar concentration from (1.0 M and 2 M). transmittance decreased by increasing from 1.0 M to 2.0 M thin films respectively. Transmissions was observed at 95%, 85% and 80% for 1.0 M, 1.5 M and 2 M respectively, α increased with increasing of molarity, The optical gap offer a decrement with the increment of molar concentration ratio from (3.55 -3.35 eV).

Acknowledgments

Authors recognize Mustansiriyah University (www. uomustansiriyah.edu.iq) for their backup.

References

1. [1] Kurbatov D., Opanasyuk A., Kshnyakina S., Melnik V. and Nesprava V., (2010). Rom. Jur. Phys., Vol. 55, p. 213–219.
2. [2] Kobayashi R., Sato N., Ichimura M. and Arai E, (2003). J. opt. and adv. mater., Vol. 5, p. 893 – 898.
3. [3] Yamamoto T., Kishimoto S. and Iida S., J. Phys., 1 (5- 6) (2001) 308–310.
4. [4] Bredol M. and Merikhi J., Mater. Sci.,33 (1998)471.
5. [5] Kavanagh Y., Alam M. J.and Cameron D.C., thin solid films, 85 (2004) 447–448.
6. [6] Contreras M. A., Nakada T., Hongo M., Pudov A. O. and Sites J. R., Proceedings 3rd World Conference of Photovoltaic Energy Conversion, Osaka, Japan, (2003) 570.
7. [7] Ben Nasr T., Kamoun N., Kanzari M.and Bennaceur R, thin solid films, 500 (2006) 4– 8.
8. [8] Jie Cheng, DongBo Fan, Hao Wang, BingWei Liu, YongCai Zhang and Hui, Chemical bath deposition of crystalline ZnS thin films, Semicond. Sci. Technol., 18 (2003) 676-679.
9. [9] Seyyed Zabihollah Rahchamani, Hamid Rezagholipour Dizaji, Mohammad Hossein Ehsani, Study of structural and optical properties of ZnS zigzag nanostructured thin films, Applied Surface Science, 356 (2015) 1096-1104.

10. [10] Inamdar AI, Sangeun Cho, Yongcheol Jo, Jongmin Kim, Jaeseok Han, Pawar SM, Hyeonseok Woo, Kalubarme RS, ChanJin Park, Hyungsang Kim, Hyunsik Im, Optical properties in Mn-doped ZnS thin films: Photoluminescence quenching, Materials Letters, 163 (2016) 126-129.
11. [11] Daniela E. Ortíz-Ramos, Luis A. González, Rafael Ramirez-Bon, p-Type transparent Cu doped ZnS thin films by the chemical bath deposition method, Materials Letters, 124 (2014) 267-270.
12. [12] Lopez M C, Espinos J P, Martin F, Leinen D and Ramos-barrado J R, Growth of ZnS thin films obtained by chemical spray pyrolysis: The influence of precursors, J. Cryst. Growth, 285 (2005) 66-75.
13. [13] Reza Sahraei, Soraya Darafarin, Preparation of nanocrystalline Ni doped ZnS thin films by ammoniafree chemical bath deposition method and optical properties, Journal of Luminescence, 149 (2014) 170-175.
14. [14] Jun Liu, Aixiang Wei, Yu Zhao, Effect of different complexing agents on the properties of chemicalbath-deposited ZnS thin films, Journal of Alloys and Compounds, 588 (2014) 228-234.
15. [15]. Reza Sahraei, , Ghaffar Motedayen Aval, Alireza Goudarzi, Compositional, structural, and optical study of nanocrystalline ZnS thin films prepared by a new chemical bath deposition route, J. Alloys Compd., 466 (2008) 488-492.
16. [16] Gode F, Gumus C and Zor M, Investigations on the physical properties of the polycrystalline ZnS thin films deposited by the chemical bath deposition method, J. Cryst. Growth, 299 (2007) 136-141.
17. [17] Aixiang Wei, Jun Liu, Mixue Zhuang, Yu Zhao, Preparation and characterization of ZnS thin films prepared by chemical bath deposition, Materials Science in Semiconductor Processing, 16 (2013) 1478–1484.
18. [18] D. H. Hwang, J. H. Ahn, K. N. Hui, K. S. Hui, and Y. G. Son, "Structural and optical properties of ZnS thin films deposited by RF magnetron sputtering," Nanoscale Research Letters, 7, (2012) 1–13,.
19. [19] J. P. Bosco, S. B. Demers, G. M. Kimball, N. S. Lewis, and H. A. Atwater, Band alignment of epitaxial ZnS/Zn3P2 heterojunctions, Journal of Applied Physics, 112 (9) (2012).
20. [20] S. Yano, R. Schroeder, H. Sakai, and B. Ullrich, "High-electricfield photocurrent in thin-film ZnS formed by pulsed-laser deposition," Applied Physics Letters, 82 (13) (2003) 2026–2028,.
21. [21] M. W. Huang, Y. W. Cheng, K. Y. Pan, C. C. Chang, F. S. Shieu, and H. C. Shih, The preparation and cathodoluminescence of ZnS nanowires grown by chemical vapor deposition," Applied Surface Science, 261(2012) 665–670.
22. [22] G. Xu, S. Ji, C. Miao, G. Liu, and C. Ye, Effect of ZnS and CdS coating on the photovoltaic properties of CuInS2-sensitized photoelectrodes, Journal ofMaterials Chemistry, 22 (11)2012 4890–4896.
23. [23] K. Nagamani, N. Revathi, P. Prathap, Y. Lingappa, and K. T. R. Reddy, "Al-doped ZnS layers synthesized by solution growth method," Current Applied Physics, 12. (2) (2012) 380–384.
24. [24] G. L. Agawane, S. W. Shin, M. S. Kim et al., "Green route fast synthesis and characterization of chemical bath deposited nanocrystalline ZnS buffer layers," Current Applied Physics, 13 (5) (2013) 850–856.
25. [25] K. Ahn, J. H. Jeon, S. Y. Jeong et al., "Chemical bonding states and atomic distribution within Zn(S,O) film prepared on CIGS/Mo/glass substrates by chemical bath deposition," Current Applied Physics, 12 (6) (2012) 1465–1469.
26. [26] O'Brien P, Otway DJ and Boyle DS, The importance of ternary complexes in defining basic conditions for the deposition of ZnS by aqueous chemical bath deposition, Thin Solid Films, 361 (362) (2000) 17-21,
27. [27] Lokhande CD, Pathan HM, Giersig M and Tributsch H, Preparation of Znx(O,S)y thin films using modified chemical bath deposition method, Appl. Surf. Sci., 187(2002) 101-107.
28. [28] Rodríguez CA, Sandoval-Paz MG, Cabello G, Flores M, Fernández H, Carrasco C, Characterization of ZnS thin films synthesized through a non-toxic precursors chemical bath, Materials Research Bulletin, 60 (2014) 313-321.
29. [29] Haddad H, Chelouche A, Talantikite D, Merzouk H, Boudjouan F, Djouadi D, Effects of deposition time in chemically deposited ZnS films in acidic solution, Thin Solid Films, 89 (2015) 451-456.
30. [30] Abdulmunem, O.M., Jabbar, A.M., Muhammad, S.K., Dawood, M.O., Chiad, S.S., Habubi, N.F., Investigation of Co-doped Cu2O thin films on the structural, optical and morphology by SPT, Journal of Physics: Conference Series,1660 (1) (2020) 012055..
31. [31] P. O'Brien and J. McAleese, Developing an understanding of the processes controlling the chemical bath deposition of ZnS andCdS, Journal ofMaterials Chemistry, 8 (11) (1998) 2309–2314.
32. [32] Eid A.H., Salim S. M., Sedik M. B., Omar H., Dahy T. and Abou elkhair H. M., Appl. Sci. Research, 6 (2010) 777-784.
33. [33] Gilbert B., Frazer B. H., Zhang H., Huang F., Banfield J. F., Haskel D., Lang J. C., Srajer G. and Stasio G. De., Phys. Rev.,.66 (2002) 245.
34. [34] Hassan, E.S., Mubarak, T.H., Chiad, S.S., Habubi, N.F., Khadayeir, A.A., Dawood, M.O., Al-Baidhany, I.A., Physical Properties of indium doped Cadmium sulfide thin films prepared by (SPT), , Journal of Physics: Conference Series 1294(2) (2019) 022008.
35. [35] Hassan, E.S., Elttayef, A.K., Mostafa, S.H., Salim, M.H., Chiad, S.S., Silver oxides nanoparticle in gas sensors applications, Journal of Materials Science: Materials in Electronics 30(17) (2019) 15943-15951.
36. [36] Hassan, E.S., Mubarak, T.H., Abass, K.H., Chiad, S.S., Habubi, N.F., Rahid, M. H, Khadayeir, A. A., Dawod M. O . and Al-Baidhany, I.A., Structural, Morphological and Optical Characterization of Tin Doped Zinc Oxide Thin Film by (SPT), Journal of Physics: Conference Series 1234(1) (2019) 012013.
37. [37] Beevi M. M., Anusuya M., Saravanan V., International Journal of Chemical Engineering and Applications, .1 (2010) 151-154.
38. [38] Khadayeir, A. A., Hassan, E. S., Chiad, S. S., Habubi, N. F., Abass, K. H., Rahid, M. H., Mubarak T. H, Dawod M. O. and Al-Baidhany, I.A., Structural and Optical Properties of Boron Doped Cadmium Oxide, Journal of Physics: Conference Series 1234 (1), 20119, 012014.

39.[39] Ali, R.S., Sharba, K.S., Jabbar, A.M., Chiad, S.S., Abass, K.H., Habubi, N.F., Characterization of ZnO thin film/p-Si fabricated by vacuum evaporation method for solar cell applications, NeuroQuantology, 18(1) (2020) 26-31.
40.[40] M. O. Dawood, S.S. Chiad, A. J. Ghazai, N. F. Habubi and O. M. Abdulmunem, Effect of Li doping on structure and optical properties of NiO nano thin-films by SPT, AIP Conference Proceedings , USA, 2213 (1) 1(2020) 020102.
41.[41] Mane RS and Lochande CD, Chemical deposition method for metal chalcogenide thin films, Mater. Chem. Phys., 65 (2000) 1-31.
42.[42] N. N. Jandow, N. F. Habubi, S. S. chiad, I. A. Al-Baidhany and M. A. Qaeed, Annealing Effects on Band Tail Width, Urbach Energy and Optical Parameters of Fe_2O_3:Ni Thin Films Prepared by Chemical Spray Pyrolysis Technique, International Journal of Nanoelectronics and Materials, 12 (1) (2019) 1-10.
43.[43] Ahmed, N.Y., Bader, B.A., Slewa, M.Y., Habubi, N.F., Chiad, S.S., Effect of boron on structural, optical characterization of nanostructured fe2o3 thin films, NeuroQuantology, 18(6), (2020) 55-60.
44.[44] Yano S, Schroeder R, Ullrich and Sakai, Absorption and photocurrent properties of thin ZnS films formed by pulsed-laser deposition on quartz, Thin Solid Films, 423 (2003) 273-276.
45.[45] Chiad, S. S. and Mubarak, T. H.,The Effect of Ti on Physical Properties of Fe_2O_3 Thin Films for Gas Sensor Applications, 2020, International Journal of Nanoelectronics and Materials, 13(2) (2020) 221-232.
46.[46] Ali, R.S., Mohammed, M.K., Khadayeir, A.A., Abood, Z.M., Habubi, N.F., Chiad, S.S., Structural and Optical Characterization of Sprayed nanostructured Indium Doped Fe2O3 Thin Films, Journal of Physics: Conference Series, 1664(1), (2020) 012016.
47.[47] Hsu CT, Epitaxial growth of II–VI compound semiconductors by atomic layer epitaxy, Thin Solid Films, 335 (1998) 284-291.
48.[48] Muhammad, S. K., Hassan, E.S., Qader, K.Y., Abass, K.H., Chiad, S. S., Habubi, N. F., Effect of vanadium on structure and morphology of SnO_2 thin films, Nano Biomedicine and Engineering, 12(1) , (2020) 67-74.
49.[49] Sakhil, M.D., Shaban, Z.M., Sharba, K.S., Habub, N.F., Abass, K.H., Chiad, S.S., Alkelaby, A.S., Influence mgo dopant on structural and optical properties of nanostructured cuo thin films, NeuroQuantology, 18 (5) (2020) 56-61.
50.[50] Khadayeir, A. A., Hassan, E. S., Mubarak, T. H., Chiad, S.S., Habubi, N. F., Dawood, M.O., Al-Baidhany, I. A., The effect of substrate temperature on the physical properties of copper oxide films, Journal of Physics: Conference Series, 1294 (2) (2019) 022009.
51.[51] Ahmed, F.S., Ahmed, N.Y., Ali, R.S., Habubi, N.F., Abass, K.H. and Chiad, S.S. Effects of Substrate Type on Some Optical and Dispersion Properties of Sprayed CdO Thin Films, NeuroQuantology, 18 (3) (2020) 56-65.
52.[52] Ghazai, A.J., Abdulmunem, O.M., Qader, K.Y., Chiad, S.S., Habubi, N.F., Investigation of some physical properties of Mn doped ZnS nano thin films, AIP Conference Proceedings 2213 (1) (2020) 020101.
53.[53] Sharba, K.S., Alkelaby, A.S., Sakhil, M.D., Abass, K.H., Habubi, N.F., Chiad, S.S., Enhancement of urbach energy and dispersion parameters of polyvinyl alcohol with Kaolin additive, NeuroQuantology, 18(3) (2020) 66-73.
54.[54] P. Kathirvel, D. Manoharan, S. M. Mohan and S. Kumar, J. Optoelectronic and Biomedical Materials, (1)(2009) 25-33.
55.JALIL, A. T., DILFY, S. H., KAREVSKIY, A., & NAJAH, N. (2020). Viral Hepatitis in Dhi-Qar Province: Demographics and Hematological Characteristics of Patients. *International Journal of Pharmaceutical Research*, *12*(1). https://doi.org/10.31838/ijpr/2020.12.01.326
56.Dilfy, S. H., Hanawi, M. J., Al-bideri, A. W., & Jalil, A. T. (2020). Determination of Chemical Composition of Cultivated Mushrooms in Iraq with Spectrophotometrically and High Performance Liquid Chromatographic. *Journal of Green Engineering*, *10*, 6200-6216.
57.Jalil, A. T., Al-Khafaji, A. H. D., Karevskiy, A., Dilfy, S. H., & Hanan, Z. K. (2021). Polymerase chain reaction technique for molecular detection of HPV16 infections among women with cervical cancer in Dhi-Qar Province. *Materials Today: Proceedings*. https://doi.org/10.1016/j.matpr.2021.05.211
58.Jalil, A. T., Kadhum, W. R., Khan, M. U. F., Karevskiy, A., Hanan, Z. K., Suksatan, W., ... & Abdullah, M. M. (2021). Cancer stages and demographical study of HPV16 in gene L2 isolated from cervical cancer in Dhi-Qar province, Iraq. *Applied Nanoscience*, 1-7. https://doi.org/10.1007/s13204-021-01947-9
59.Widjaja, G., Jalil, A. T., Rahman, H. S., Abdelbasset, W. K., Bokov, D. O., Suksatan, W., ... & Ahmadi, M. (2021). Humoral Immune mechanisms involved in protective and pathological immunity during COVID-19. *Human Immunology*. https://doi.org/10.1016/j.humimm.2021.06.011
60.Moghadasi, S., Elveny, M., Rahman, H. S., Suksatan, W., Jalil, A. T., Abdelbasset, W. K., ... & Jarahian, M. (2021). A paradigm shift in cell-free approach: the emerging role of MSCs-derived exosomes in regenerative medicine. *Journal of Translational Medicine*, *19*(1), 1-21. https://doi.org/10.1186/s12967-021-02980-6
61.Hanan, Z. K., Saleh, M. B., Mezal, E. H., & Jalil, A. T. (2021). Detection of human genetic variation in VAC14 gene by ARMA-PCR technique and relation with typhoid fever infection in patients with gallbladder diseases in Thi-Qar province/Iraq. *Materials Today: Proceedings*. https://doi.org/10.1016/j.matpr.2021.05.236
62.Saleh, M. M., Jalil, A. T., Abdulkereem, R. A., & Suleiman, A. A. Evaluation of Immunoglobulins, CD4/CD8 T Lymphocyte Ratio and Interleukin-6 in COVID-19 Patients. *TURKISH JOURNAL of IMMUNOLOGY*, *8*(3), 129-134. https://doi.org/10.25002/tji.2020.1347
63.Turki Jalil, A., Hussain Dilfy, S., Oudah Meza, S., Aravindhan, S., M Kadhim, M., & M Aljeboree, A. (2021). CuO/ZrO2 nanocomposites: facile synthesis, characterization and photocatalytic degradation of tetracycline antibiotic. *Journal of Nanostructures*.

64. Sarjito, Elveny, M., Jalil, A., Davarpanah, A., Alfakeer, M., Awadh Bahajjaj, A. & Ouladsmane, M. (2021). CFD-based simulation to reduce greenhouse gas emissions from industrial plants. *International Journal of Chemical Reactor Engineering*, (), 20210063. https://doi.org/10.1515/ijcre-2021-0063
65. Marofi, F., Rahman, H. S., Al-Obaidi, Z. M. J., Jalil, A. T., Abdelbasset, W. K., Suksatan, W., ... & Jarahian, M. (2021). Novel CAR T therapy is a ray of hope in the treatment of seriously ill AML patients. *Stem Cell Research & Therapy*, *12*(1), 1-23. https://doi.org/10.1186/s13287-021-02420-8
66. Jalil, A. T., Shanshool , M. T. ., Dilfy, S. H. ., Saleh, M. M., & Suleiman, A. A. . (2021). HEMATOLOGICAL AND SEROLOGICAL PARAMETERS FOR DETECTION OF COVID-19. *Journal of Microbiology, Biotechnology and Food Sciences*, e4229. https://doi.org/10.15414/jmbfs.4229
67. Vakili-Samiani, S., Jalil, A. T., Abdelbasset, W. K., Yumashev, A. V., Karpisheh, V., Jalali, P., ... & Jadidi-Niaragh, F. (2021). Targeting Wee1 kinase as a therapeutic approach in Hematological Malignancies. *DNA repair*, 103203. https://doi.org/10.1016/j.dnarep.2021.103203
68. NGAFWAN, N., RASYID, H., ABOOD, E. S., ABDELBASSET, W. K., Al-SHAWI, S. G., BOKOV, D., & JALIL, A. T. (2021). Study on novel fluorescent carbon nanomaterials in food analysis. *Food Science and Technology*. https://doi.org/10.1590/fst.37821
69. Marofi, F., Abdul-Rasheed, O. F., Rahman, H. S., Budi, H. S., Jalil, A. T., Yumashev, A. V., ... & Jarahian, M. (2021). CAR-NK cell in cancer immunotherapy; A promising frontier. *Cancer Science*, *112*(9), 3427. https://doi.org/10.1111/cas.14993
70. Abosaooda, M., Wajdy, J. M., Hussein, E. A., Jalil, A. T., Kadhim, M. M., Abdullah, M. M., ... & Almashhadani, H. A. (2021). Role of vitamin C in the protection of the gum and implants in the human body: theoretical and experimental studies. *International Journal of Corrosion and Scale Inhibition*, *10*(3), 1213-1229. https://dx.doi.org/10.17675/2305-6894-2021-10-3-22
71. Jumintono, J., Alkubaisy, S., Yánez Silva, D., Singh, K., Turki Jalil, A., Mutia Syarifah, S., ... & Derkho, M. (2021). Effect of Cystamine on Sperm and Antioxidant Parameters of Ram Semen Stored at 4° C for 50 Hours. *Archives of Razi Institute*, *76*(4), 923-931. https://dx.doi.org/10.22092/ari.2021.355901.1735
72. Roomi, A. B., Widjaja, G., Savitri, D., Turki Jalil, A., Fakri Mustafa, Y., Thangavelu, L., ... & Aravindhan, S. (2021). SnO2: Au/Carbon Quantum Dots Nanocomposites: Synthesis, Characterization, and Antibacterial Activity. *Journal of Nanostructures*.
73. Raya, I., Chupradit, S., Kadhim, M. M., Mahmoud, M. Z., Jalil, A. T., Surendar, A., ... & Bochvar, A. N. (2021). Role of Compositional Changes on Thermal, Magnetic and Mechanical Properties of Fe-PC-Based Amorphous Alloys. *Chinese Physics B*. https://doi.org/10.1088/1674-1056/ac3655
74. Chupradit, S., Jalil, A. T., Enina, Y., Neganov, D. A., Alhassan, M. S., Aravindhan, S., & Davarpanah, A. (2021). Use of Organic and Copper-Based Nanoparticles on the Turbulator Installment in a Shell Tube Heat Exchanger: A CFD-Based Simulation Approach by Using Nanofluids. *Journal of Nanomaterials*. https://doi.org/10.1155/2021/3250058
75. Raya, I., Chupradit, S., Mustafa, Y., H. Oudaha, K., M. Kadhim, M., Turki Jalil, A., J. Kadhim, A., Mahmudiono, T., Thangavelu, L. (2021). Carboxymethyl Chitosan Nano-Fibers for Controlled Releasing 5-Fluorouracil Anticancer Drug. *Journal of Nanostructures*,